Depletion Interactions: Effects of Added Homopolymer on Ordered Phases Formed by Spherical Block Copolymer Micelles

Sayeed Abbas[†] **and Timothy P. Lodge***[,†,‡]

Departments of Chemical Engineering & Materials Science and Chemistry, University of Minnesota, Minneapolis, Minnesota 55455

Received June 19, 2008; Revised Manuscript Received September 9, 2008

ABSTRACT: Three distinct poly(styrene-*b*-isoprene) (SI) diblock copolymers with molecular weights of 16−16, 38−14, and 50−13 kDa for styrene and isoprene, respectively, formed spherical micelles when dissolved in diethyl phthalate (DEP). Since DEP is a styrene-selective solvent, micelles with polyisoprene in the core and polystyrene in the corona were formed. At block copolymer concentrations of 20%, 16%, and 14% in DEP, the spherical micelles of SI(16−16), SI(38−14), and SI(50−13) pack onto a face-centered cubic (FCC) lattice, a mixture of FCC and body-centered cubic (BCC) lattices, and a BCC lattice, respectively. Polystyrene homopolymers with molecular weights of 4, 48, and 180 kDa were added to these ordered solutions. The following general trends were observed: the FCC phase tended to disorder, and samples that originally behaved like soft solids exhibited liquidlike flow behavior. The effect increased strongly with both the molecular weight and concentration of homopolymer in the solution. Furthermore, the BCC lattice tended to be displaced by the FCC lattice, or to disorder, when homopolymer was added. These results can be explained by invoking depletion interactions, which have been studied extensively in colloid/polymer mixtures. However, the phenomenon differs in certain details from colloidal systems because the addition of homopolymer can also influence the aggregation number of the micelles, which in turn affects the lattice packing of the micelles.

Introduction

Self-assembly of diblock copolymers in selective solvents offers a rich array of nanostructures with diverse applications. In dilute solutions an AB diblock copolymer self-assembles in an A-selective solvent to form a spherical micelle with A in the corona and B in the core. Other micelle morphologies are also possible, and by proper choice of block copolymer composition, solvent, and temperature, one can control the micelle morphology. Detailed reviews on this subject are available.[1,2] When the concentration of spherical micelles is increased in solution to approximately 10−20%, the micelles pack onto either a face-centered cubic (FCC) or body-centered cubic (BCC) lattice.[3−12] In some cases the A15[13,14] and LS_{13} superlattice[15,16] structures have also been reported. The primary factors controlling the phase behavior of a diblock copolymer in a selective solvent include temperature, polymer concentration, and volumetric composition of the diblock.[4] The aim of this work is to examine how the introduction of homopolymer affects the behavior of cubic phases formed by spherical micelles and thereby to introduce a new control parameter in the self-assembly of diblock copolymers.

Qualitatively, the addition of homopolymer to micelle solutions is similar to depletion interactions in colloidal systems.[17−20] When homopolymer is added to a solution of colloidal particles, the polymer coils are excluded from a region close to the surface of the sphere due to the high entropic penalty for conformational distortion. Thus, a depletion layer as thick as the radius of gyration (R_g) of the polymer coils in the solution develops around each sphere. When the spheres are far apart from each other, a uniform concentration gradient of the polymer exists from the bulk to the surface of the spheres, resulting in an isotropic osmotic force of the polymer coils on the particle. If two spheres approach one another and the depletion layers overlap, the polymer coils are excluded from the overlapping region. This leads to an anisotropic osmotic pressure, and an effective attraction develops between the colloid particles.

In contrast to colloidal particles, micelles offer an additional level of self-assembly: the process of micellization itself. Hence, the effect of depletion interactions can be even more subtle. Relatively little work has been done to study the effect of addition of homopolymers to diblock copolymers in a selective solvent. The earliest study to investigate this effect was performed by Watanabe and Kotaka on poly(styrene-*b*-butadiene) (SB) in tetradecane,[21] where the diblock copolymer self-assembles to form spherical micelles with polystyrene (S) in the core and polybutadiene (PB) in the corona. Above a critical concentration of SB, an ordered phase exhibiting plastic flow under steady shear was formed. When PB was added, the solution lost its plasticity. Similar results were reported when homopolymer poly(ethylene oxide) (PEO) was added to soft solids formed by pluronic polymers in water.[22] It was observed that with moderate molecular weight PEO the gel melted, whereas with high molecular weight PEO phase separation occurred. In both these papers, no scattering experiments were reported to characterize the morphology of the soft solids. Homopolymer PEO was also added to ordered phases formed by dissolving hydrophobically end-capped PEO chains in water,[23−25] and similar results were obtained. By performing SAXS, the micelles were shown to pack on BCC lattice, which disordered upon addition of homopolymer.[23] In addition, Yamazaki et al. performed self-consistent field theory calculations, which showed that upon increasing PEO molecular weight the homopolymer was excluded from the corona of the micelles.[24]

The behavior of multiarmed stars is also similar to micelles, and several recent studies have focused on multiarm star polymers with added homopolymer in solution. It was observed that with addition of homopolymer the soft solid melted.[26] The dynamics of the system was investigated by rheology[27] and photon correlation spectroscopy;[28] the results revealed that addition of homopolymer can significantly alter the phase behavior of soft spheres. We have previously reported results from small-angle neutron scattering experiments on micelle/

* Author for correspondence: E-mail lodge@umn.edu.
† Department of Chemical Engineering & Materials Science.
‡ Department of Chemistry.

10.1021/ma8013838 CCC: $40.75
Published on Web 10/22/2008

Table 1. Polymer Characterization

polymer	M_N (g/mol)[a]	(first block M_N−second block M_W)	PDI (M_W/M_N)[a,b]
SI(16−16)	32 000	16 000−16 000	1.01
SI(38−14)	52 000	38 000−14 000	1.02
SI(50−13)	63 000	50 000−13 000	1.01
S(4)	4 000		1.02
S(48)	48 000		1.01
S(180)	178 000		1.01

[a] M_N and M_W represent number-average and weight-average molecular weight, respectively, as measured by SEC and ^{1}H NMR. [b] Polydispersity index (M_W/M_N) of the synthesized block copolymer as determined by SEC using the light scattering detector.

homopolymer mixtures, showing the presence of effective attractive forces between micelles.[29] We further showed that due to the addition of homopolymer, the aggregation number (N_{agg}) of the micelles increased slightly. These experiments focused on disordered dilute or semidilute solutions. Here we consider the effect of addition of homopolymer on ordered phases, particularly on the face-centered cubic (FCC) and body-centered cubic (BCC) lattices. The results are interpreted in terms of depletion interactions.

Experimental Section

Materials. Poly(styrene-*b*-isoprene) (SI) was synthesized by living anionic polymerization using standard procedures.[3] Monomers styrene and isoprene were obtained from Sigma Aldrich and further purified. Styrene was stirred over calcium hydride overnight and further stirred over dibutylmagnesium for 8 h. Isoprene was stirred over calcium hydride overnight and then subsequently stirred for 4 h over *n*-butyllithium and dibutylmagnesium. After purification the monomers were vacuum-distilled into burets. The polymerization was initiated by injecting *sec*-butyllithium into a mixture of styrene and cyclohexane at 40 °C. Subsequently, the solution was stirred for 4 h at 40 °C, after which isoprene was added, and the reaction was allowed to run for an additional 4 h at 40 °C. Degassed methanol was used for termination. The reaction mixture was then washed with water, and the product was collected by precipitating the polymer in a 50/50 mixture of isopropanol and methanol. Size exclusion chromatography (SEC) with both refractive index (Wyatt Optilab) and light scattering (Wyatt Dawn) detectors was used to determine the molecular weight of the first block (polystyrene). Using ^{1}H NMR spectroscopy, the composition of the diblock was determined, from which the molecular weight of the second block (isoprene) was also calculated. Homopolymer polystyrene (S) with different molecular weights was also synthesized via the same protocol. Hereafter, the poly(styrene-*b*-isoprene) diblocks and polystyrene homopolymer will be abbreviated as SI(x−y) and S(x), where x and y represents the molecular weight of polystyrene and polyisoprene, respectively, in kDa. Table 1 shows the characterization results for the synthesized polymers. The solvent diethyl phthalate (DEP) and cosolvent methylene chloride were obtained from Sigma-Aldrich and used without further purification.

Sample Preparation. All samples were prepared gravimetrically with the aid of methylene chloride as the cosolvent. Typically, the polymer + cosolvent mixture was stirred for 24 h, after which the cosolvent was removed by evaporation until a constant weight of the vial was achieved. The concentration of polymer was converted to volume percent by taking the densities of polystyrene, polyisoprene, and DEP to be 1.05, 0.913, and 1.118 g/mL, respectively. A sample denoted as x% SI + y% S contains x vol % diblock SI and y vol % homopolymer S.

Small-Angle X-ray Scattering. Small-angle X-ray scattering (SAXS) was performed on beamline 5 ID-D in the Du Pont−Northwestern−Dow (DND-CAT) station at the Advanced Photon Source, Argonne National Laboratory. The energy of the radiation was either 17 keV (λ = 0.73 Å) or 12 keV (λ = 1.033 Å). An undulator was used as an insertion device. The energy was selected by a double crystal monochromator, and further beam collimation was achieved by two adjustable square slits. The temperature was varied by using a Linkam temperature stage. 2D SAXS images were obtained by using the MAR CCD camera with an active diameter of 133 mm and maximum resolution of 2048 × 2048 pixels. The sample-to-detector distance was varied from 3 to 9 m. Silver behenate or a block copolymer with known domain spacing was used as wave vector calibrants. SAXS experiments were also conducted on the Characterization Facility beamlines at the University of Minnesota. Cu Kα X-rays (λ = 1.54 Å) are generated by a Rigaku RTU-200BVH rotating anode X-ray generator. Franks mirror optics were used to focus the beam on a 1024 × 1024 pixel HI-STAR Siemens area detector. A sample-to-detector distance of either 2 or 6 m was used.

Table 2. Homopolymer:Micelle Size Ratio (α)

	R_h (nm)	S(4)	S(48)	S(180)
SI(16−16)	20	<0.1	0.26	0.61
SI(38−14)	20	<0.1	0.26	0.61
SI(50−13)	27	<0.1	0.19	0.46

Rheology. Rheological experiments were performed on an ARES instrument (Rheometric Scientific) by using parallel plates 25 mm in diameter with gap widths ranging from 0.6 to 1.2 mm. Temperature was controlled by a nitrogen convection oven. Since the boiling point of DEP is ∼300 °C and temperatures never exceeded 130 °C during the experiments, loss of solvent due to evaporation was negligible. The strain amplitudes were carefully chosen such that the experiments were performed in the linear viscoelastic regime. Measurements at a fixed frequency and strain and as a function of temperature were performed to determine the order−disorder transition (ODT) and order−order transition (OOT) temperature of the solutions. Generally, the frequency employed for the measurements was 1 rad/s and the temperature ramp rate was 1 °C/min. The dynamic moduli (G' and G'') were also measured by frequency sweep measurements at a fixed strain of 1%.

Dynamic Light Scattering. Dynamic light scattering (DLS) was used to determine the hydrodynamic (R_h) radii of SI micelles and S homopolymer in DEP. The DLS instrument consisted of a Lexel 95-2 Ar^+ laser operating at 488 nm, a home-built goniometer, a Brookhaven BI-DS photomultiplier, an electrically heated silicon oil bath, and a Brookhaven BI-9000 correlator. The intensity autocorrelation functions were measured at three angles (60°, 90°, and 120°). Cumulant expressions were used to fit the autocorrelation functions, and the mean decay constant ($\bar{\Gamma}$) obtained from each fit was utilized in the Stokes−Einstein equation to calculate R_h. All measurements were performed on dilute 1% polymer solutions at 25 °C. The R_h values were used to estimate the size ratio of homopolymer:micelle (α), as summarized in Table 2. We observe in Table 2 that α is the same for SI(16−16) and SI(38−14). This occurs because R_h of both SI(16−16) and SI(38−14) micelles in DEP is ∼20 nm. This result can be rationalized by noting that although the molecular weight of core block is approximately the same in both diblocks, the corona block of SI(38−14) is longer, thus driving down the aggregation number (N_{agg}). In SI(16−16), N_{agg} is large but the corona is thinner. The changes in these two parameters balance each other, and hence the values of R_h remain approximately the same.

Results

All three diblock copolymers SI(16−16), SI(38−14), and SI(50−13) form spherical micelles when dissolved in dilute solution in diethyl phthalate (DEP). Since DEP is a selective solvent for polystyrene, the micelles have polyisoprene in the core and polystyrene in the corona. Ordered phases are obtained when the concentration of the micelles is increased in solution. The morphology of the solutions was characterized by small-angle X-ray scattering (SAXS). The sample 20% SI(16−16) is face-centered cubic (FCC), 16% SI(38−14) shows a mixture of FCC and body-centered cubic (BCC), and 14% SI(50−13) has only the BCC phase. The selection of FCC−BCC phases in micelle systems was first investigated by Gast et al., who

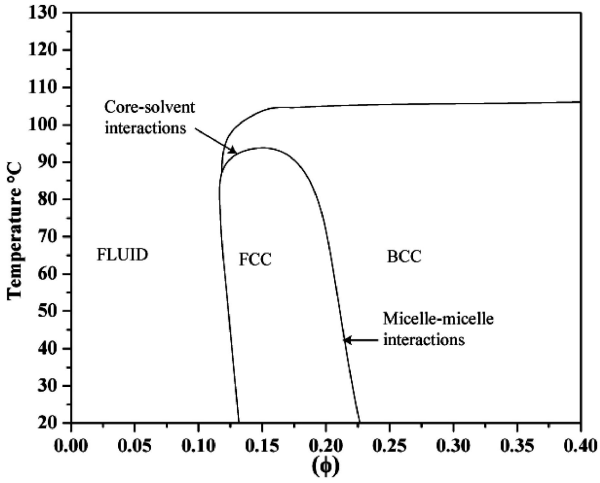

Figure 1. A representative phase diagram for a symmetric diblock copolymer derived from calculations performed by Grason,[27] showing the general idea of phase transitions among FCC and BCC lattices. Two types of FCC−BCC transitions occur: (i) a thermotropic transition driven by core−solvent interactions; (ii) a lyotropic transition driven by micelle−micelle interactions.

speculated that the ratio of corona height (R_{corona}) to core radius (R_{core}) determines the structure formed in solution.[6] From experiments, a critical value of $R_{corona}/R_{core} \approx 1.5$ was inferred, above which the FCC → BCC transition occurred. However, experiments later showed that with R_{corona}/R_{core} as high as 2.4 the FCC phase could still be formed by micelles.[16] Furthermore, Lodge et al. reported thermotropic FCC−BCC transitions which were driven by a reduction in solvent selectivity with temperature.[4] A more comprehensive understanding of this phenomenon later emerged from theoretical calculations performed by Grason.[30] A representative phase diagram derived from the calculations is shown in Figure 1.

According to Grason, the interplay between FCC and BCC is not governed solely by the ratio R_{corona}/R_{core}; rather, the origin of the transitions can be traced back to two driving forces: (i) core−solvent interactions and (ii) micelle−micelle interactions. Both these two factors influence the number density of micelles in solution. At relatively low micelle number density in solution, the micelles interact through the long-ranged part of the intermicelle potential and the FCC phase is favored because of more distant nearest neighbors in the unit cell. However, as micelle number density increases, the micelles overlap more and start interacting through the short-ranged logarithmic component of the intermicelle potential, and in this scenario the BCC lattice is generically favored.[30] The strength and range of interactions are important factors which decide the choice of lattice,[31] and they in turn are linked to micelle number density and aggregation number. In Figure 1, the thermotropic FCC−BCC transition is driven by a decrease in solvent selectivity with temperature.[5] Neutron scattering results show that the aggregation number decreases due to a decrease in solvent selectivity, thereby increasing the micelle number density in solution. Hence, near the order−disorder boundary, the BCC phase is observed. Calculations by Grason also predict lyotropic FCC−BCC transitions, which have been observed experimentally in SI[32] and poly(styrene-*b*-dimethylsiloxane) (SD) + DEP systems.[33] In this case, the increased micelle overlap decreases the aggregation number and forces the rearrangement of the lattice from FCC to BCC. Our goal therefore is to study the effects of addition of homopolymer to the FCC and BCC phases and explore how the presence of homopolymer influences the transitions between these two ordered phases.

Homopolymer polystyrene was added to the cubic lattices, and by varying the concentration of the homopolymers from 2 to 6%, the effect of added homopolymer was investigated. The results at room temperature are summarized in Table 3.

From Table 3, we observe three patterns of morphological change upon addition of homopolymer: (a) FCC → disordered; (b) BCC → FCC → disordered; (c) BCC → disordered. The results depend on the concentration and molecular weight of the added homopolymer. The effects on FCC and BCC phases will be discussed below separately.

Effect on FCC Phase. At 25 °C SI(16−16) micelles pack onto an FCC lattice. The FCC phase remained unaltered upon addition of S(4), whereas when S(48) was added, the FCC lattice was disordered. Figure 2 shows 1D SAXS patterns from some of the samples with S(48) at 25 °C. The higher order peaks were considerably weakened in the sample 20% SI(16−16) + 4% S(48), and on further increasing the S(48) concentration to 6%, the sample was completely disordered. Even though in Figure 2 we only show data corresponding to the SI(16−16) + S(48) samples, from Table 3 we observe that the disordering of the ordered phase occurs universally in all samples. The molecular weight and concentration of homopolymer play an important role in this phenomenon. Rheology was also performed to characterize the flow behavior of the samples. As shown in Figure 3, the frequency response of the 20% SI(16−16) sample is typical of a soft solid where the elastic modulus (G') remains almost constant as a function of frequency. With added low molecular weight homopolymer S(4), the frequency response remains unchanged. When 2% of S(48) was added, the G' changed considerably as a function of frequency, indicating the melting of the solid. When the concentration was further increased to 4% S(48), the torque fell below the transducer's minimum limit, and hence measurements could not be made. The rheological response observed in this system is very similar to previous results obtained from multiarm stars[26] and micelles.[21,22] The SAXS and rheology results displayed here clearly show that the melting of the soft solid is simultaneously accompanied by a loss of long-range order in the sample.

We infer that the driving force behind the disordering of the lattice is depletion interactions. We previously performed small-angle neutron scattering experiments (SANS) on a semidilute solution (concentration ≈ 10%) of poly(styrene-*b*-deuterated isoprene) (SdI) micelles in DEP.[29] The molecular weights of the styrene and deuterated isoprene blocks were 15 and 14 kDa, respectively. With addition of homopolymer, an increase in $I(q)$ was observed at low q. As the scattering intensity was dominated by deuterated micellar cores, this indicates the presence of attractive interactions between micelles, thereby implicating depletion interactions in micelle/homopolymer mixtures. These core-contrast data were also fitted to the Asakura−Oosawa (AO) model, which has been used in the literature to fit SANS data from colloid/polymer mixtures.[34,35] Micelles typically interact via a soft repulsive potential, with the steepness varying with the structure of the micelle.[36,37] When the number density of micelles is increased, the repulsive intermicellar interactions restrict the local free volume available for these micelles to move. Thus, the free energy of the system is minimized when the micelles pack on a lattice to reduce unfavorable micelle−micelle overlap. With the introduction of depletion forces in the system, a short-ranged attraction develops between micelles, as a result of which the net effective repulsions between the micelles are compensated.[26,38,39] Thus, the micelles lose the driving force to pack on to an ordered lattice, and a disordered fluid can be favored over the ordered phase. Presumably this disordering process is largely independent of the symmetry of the initial ordered phase morphology. Evidence for this hypothesis can be found in Table 3, where both FCC and BCC lattices tend to disorder upon addition of homopolymer.

Table 3. Morphology of Samples Measured by SAXS at 25 °C[a,b,c]

	S(4)				S(48)			S(180)		
	0%	2%	4%	6%	2%	4%	6%	2%	4%	6%
SI(16−16)	FCC	FCC	FCC	FCC	FCC	FCC	DIS	−	−	−
SI(38−14)	FCC+BCC	FCC+BCC	FCC+BCC	FCC+BCC	FCC	FCC	DIS	DIS	DIS	DIS
SI(50−13)	BCC	BCC	BCC	BCC	BCC	BCC	DIS	FCC	DIS	DIS

[a] DIS denotes the samples are disordered. [b] − signifies that the samples are macrophase separated. [c] The concentration of SI(16−16), SI(38−14), and SI(50−13) was kept fixed at 20, 16, and 14%, respectively.

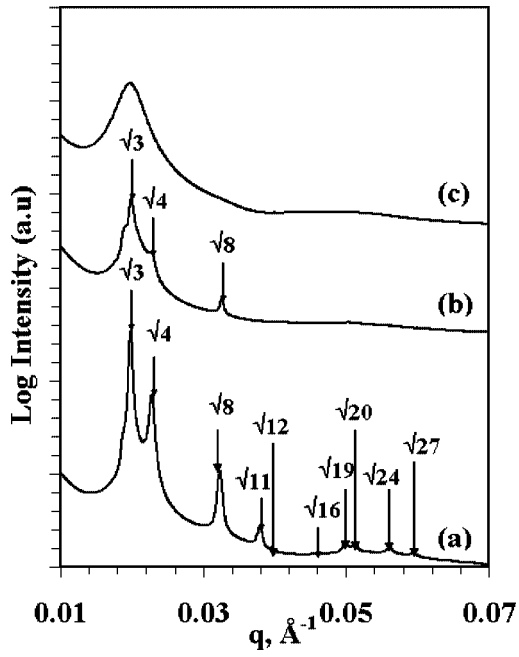

Figure 2. 1D SAXS pattern from (a) 20% SI(16−16), (b) 20% SI(16−16) + 4% S(48), and (c) 20% SI(16−16) + 6% S(48). All scattering patterns were obtained at 25 °C.

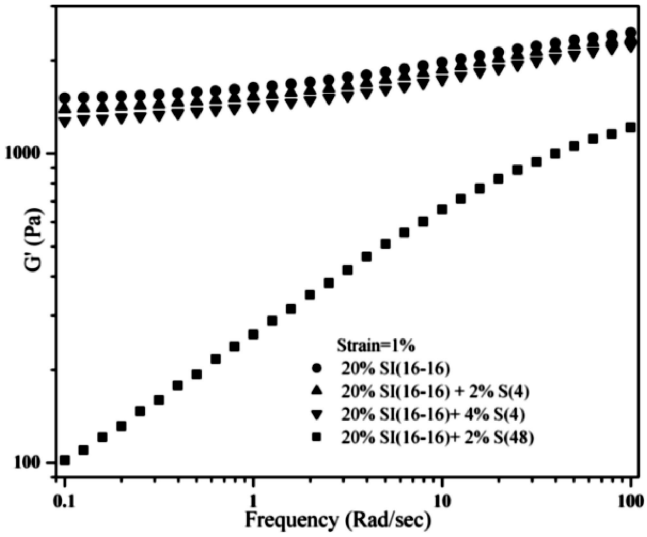

Figure 3. Frequency sweep response of samples with S(4) and S(48) homopolymer added. With 2% and 4% of S(4), the frequency sweep response of the samples remained almost unaltered. When 2% of S(48) was added, the elastic modulus (G') decreased as a function of frequency, indicating the melting of the soft solid. Temperature was 30 °C.

The molecular weight and concentration of the homopolymer play an important role as well. The range and the strength of the attractive force depend on the size ratio of homopolymer to particle (α) and concentration of the free polymer (c), respectively.[19] If α becomes too large, the attractive force generated between the micelles leads to phase separation of the micelles and homopolymer. Samples of 20% SI(16−16) + S(180) were optically opaque, whereas all other samples in Table 3 were clear, from which we concluded that phase separation had occurred in these samples. As reported in Table 2, the value of α for the SI(16−16) + S(180) system is 0.61. Interestingly, although α for 16% SI(38−14) + S(180) samples is 0.61, those samples do not show any sign of macrophase separation. There can be at least two reasons behind this result: (i) In terms of micelle number density and concentration, 20% SI(16−16) will not be equivalent to 16% SI(38−14), and thus the net effective attractive force developed between the micelles may be different. However, it must be pointed out here that the concentrations of SI(16−16) and SI(38−14) were chosen so that they were approximately equidistant from the order−disorder boundary at room temperature.[4,40] (ii) The SI(38−14) micelles have a relatively longer corona than SI(16−16), and hence the S(180) chains overlap more with the coronal brush of SI(38−14). The overlapping of chains could reduce the attractive force developed between the micelles. Evidence of chain overlap and shrinkage of coronal chains was obtained by fitting the neutron scattering data from SdI(15−14) micelles.[29] The chain overlap screens the excluded volume interactions in the corona, as a result of which the coronal brush shrinks. The height of the corona (R_{cor}) decreased upon addition of homopolymer; the higher the molecular weight of homopolymer, the more the corona contracted.

However, experiments performed in this paper do not reveal the location of the homopolymer in the lattice or quantify the degree of overlap between the corona and homopolymer. Neutron reflectivity experiments[41−43] and self-consistent field theory calculations[44] on tethered polymer + free homopolymer chains show that one of the parameters influencing the degree of overlap between them is the molecular weight of the free chains. With higher molecular weight, the free chains penetrate less. Self-consistent field theory calculations on a micelle + homopolymer system also support the same result.[24] The calculations also show the corona chains shrink more when the molecular weight of homopolymer is higher, and the high molecular weight free chains are primarily located in the interstitial region of the lattice.

Effect on BCC Phase. Micelles are distinct from uncharged sterically stabilized colloidal systems because soft intermicellar interactions enable the formation of BCC phases in solution. The micelles in the sample 12% SI(50−13) pack onto a BCC lattice. When 2% S(180) is added to the solution, the BCC is replaced by a FCC phase. Further confirmation of this novel result was obtained from the phase behavior of SI(38−14). In the sample 16% SI(38−14), the micelles packed on to a mixture of FCC and BCC phases, but with the addition of 2% S(48), the coexistent BCC phase disappeared and the micelles pack exclusively onto an FCC lattice.

To understand these results, recall that the driving force behind the FCC−BCC transition is micelle number density, which in turn is linked to the aggregation number (N_{agg}) of the micelles.[5] When N_{agg} is low, the number density of micelles is high and the intermicellar interactions are softer, as a result of which BCC lattices are preferred. From the scattering patterns we can locate the primary peak (q^*), from which one can

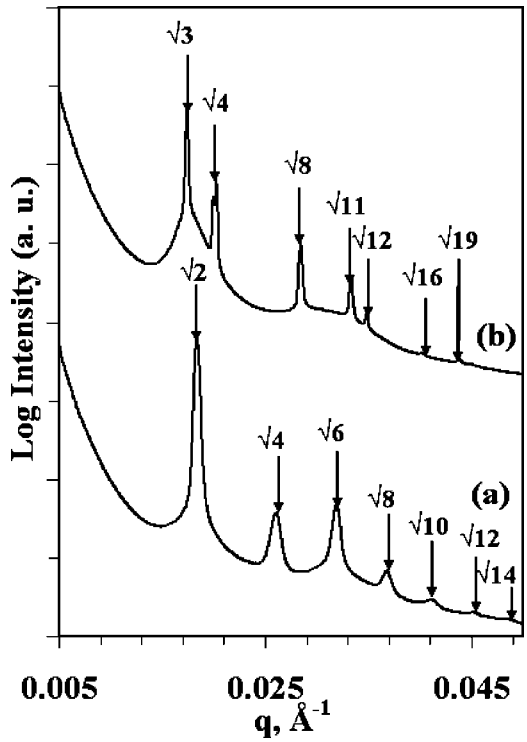

Figure 4. 1D SAXS patterns of the samples (a) 14% SI(50−13) and (b) 14% SI(50−13) + 2% S(180). All scattering patterns were obtained at 25 °C.

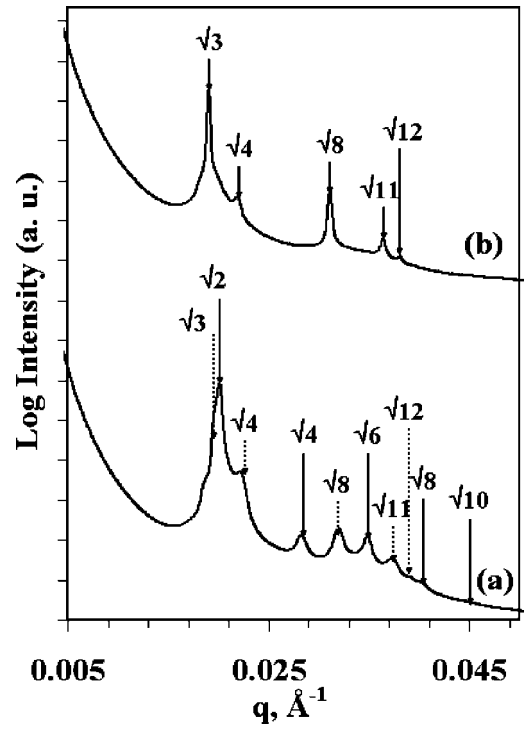

Figure 5. 1D SAXS patterns of the samples (a) SI(38−14) 16%. The dashed and solid lines indicate indexing on FCC and BCC, respectively. (b) 16% SI(38−14) + 2% S(48). All scattering patterns were obtained at 25 °C.

calculate a nearest-neighbor radius of a micelle (R_{mic}) from the equation

$$R_{mic} = \frac{\sqrt{6}}{4}\frac{2\pi}{q^*} \quad (1)$$

From the 1D scattering data shown in Figure 4, we observe that the primary peak position (q^*) is at 0.0184 and 0.0174 Å^{-1} in the samples 12% SI (50−13) (BCC) and 12% SI(50−13) + 2% S(180) (FCC), respectively. In the samples 16% SI (38−14) we have a mixture of FCC and BCC. From Figure 5, q^* of the FCC and BCC phases in the sample SI(38−14) 16% is located at 0.0195 and 0.0201 Å^{-1}, respectively. In the sample SI(38−14) + 2% S(48), q^* of the FCC phase is located at 0.019 Å^{-1}. Thus, we observe that q^* of samples with FCC is consistently smaller than those with BCC, thereby indicating that micelles packing on FCC lattices have a larger R_{mic} and hence larger N_{agg}. Grason showed theoretically that a decrease in micelle number density and increase in N_{agg} leads to an order−order transition from BCC to FCC.[30] Furthermore, the shrinkage of the corona makes the intermicellar interactions harder and the micelle behave more like hard spheres, thereby favoring the FCC lattice more. Thus, we can conclude that addition of homopolymer drives up N_{agg} and makes intermicellar interactions harder, as a result of which the FCC lattice is preferred over the BCC phase. With further addition of S(48) or S(180) in the samples of SI(38−14) and SI(50−13), the FCC lattices are disordered. This result has already been discussed in the previous section. Recently, similar results were obtained by Mortensen et al., who reported the effects of diblock PEO−PPO impurity on the phase behavior of a pluronic (F127) PEO−PPO−PEO + water system.[45] The authors observed that a 20% pristine pluronic (PEO−PPO−PEO) triblock forms a BCC phase in aqueous solutions at 50 °C, but upon addition of the diblock impurity at the same temperature, the BCC lattice is replaced by an FCC phase. By performing chromatography experiments, the authors further show that the diblocks are not incorporated within the triblock micelles and most probably exist as free chains in the solution.

The increase in N_{agg} due to addition of homopolymer can be rationalized if we consider the free energy balance of a diblock copolymer chain in a micelle. There are three contributions to the total free energy of the chain in the micelle: chain stretching in core, interfacial tension at core/corona interface, and chain stretching in corona.[46,47] Of these three contributions, the interfacial tension favors an increase in N_{agg} to reduce the net surface area available per chain in the micelle. But when N_{agg} increases, the chains in the core and corona stretch more, and thus the final N_{agg} is obtained by a balance of these three contributions. Once homopolymer is added to the solution, the homopolymer chains screen the excluded volume interactions in the corona and the coronal brush shrinks. As a result, the contribution of the interfacial tension to the free energy gathers more significance and hence N_{agg} increases. This result was also obtained by a simple scaling analysis by Halperin.[48]

In the SI + DEP system, an FCC−BCC order−order transition (OOT) also occurs at higher temperature. When the sample 20% SI(16−16) is heated, a mixture of FCC and BCC phase is observed at 90 °C. On further heating, the FCC phase is completely replaced by BCC, and finally the sample disorders at 105 °C. When S(48) is progressively added to the sample, the order−disorder transition (ODT) temperature (T_{ODT}) decreases and the OOT temperature (T_{OOT}) increases. The net result is that the high-temperature BCC window is squeezed out of the phase diagram. Figure 6 shows the progressive change in T_{OOT} and T_{ODT} with addition of homopolymer. The data were obtained by a combination of SAXS and rheology, and the data underlying Figure 6 are given in the Supporting Information. The OOT from FCC to BCC occurs primarily due to core block−solvent interactions. At higher temperatures, the selectivity of solvent decreases as a result of which N_{agg} decreases and the micelle number density increases. In this scenario the micelles pack on to a BCC lattice. With addition of homopoly-

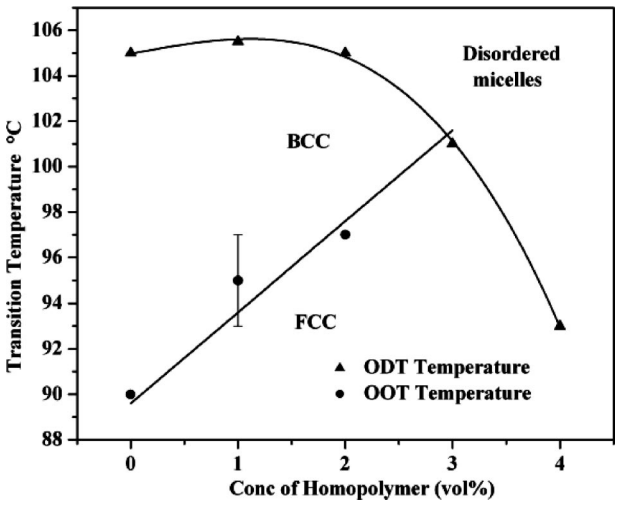

Figure 6. With progressive addition of S(48), the OOT temperature increases and ODT temperature decreases as a result of which the BCC window disappears from the phase diagram. The concentration of SI(16−16) was kept fixed at 20%.

mer, N_{agg} increases and prevents the micelles from packing onto a BCC lattice. For example, the q^* for the FCC phase occurring at 90 °C in the samples 20% SI(16−16), 20% SI(16−16) + 2% S(48), and 20% SI(16−16) + 4% S(48) are at 0.022 18, 0.020 85, and 0.0207 Å^{-1}, respectively. Using eq 1, we observe that R_{mic} values increase with addition of homopolymer, thereby indicating an increase in N_{agg}.

The reduction of the ODT temperature also plays a key role in eliminating the BCC structure from the phase map. A sharp drop in T_{ODT} starts from ~2.0% of S(48). A possible explanation to this T_{ODT} drop can be obtained if we consider the effective concentration of homopolymer in these solutions. An indication of the onset of chain overlap in good solvents can be obtained from the equation

$$c^* = \frac{3M_w}{4\pi R_g{}^3 N_{av}} \tag{2}$$

where R_g is the radius of gyration of the homopolymer in the solvent, M_w is the molecular weight, and N_{av} is Avogadro's number. For good solvents, $R_g \sim N^{0.589}$, where N is the number of repeat units in the polymer. By substituting this relation in eq 2, we get $c^* \sim N^{-0.767}$, whereas a scaling of $c^* \sim N^{-0.73}$ can been obtained from c^* vs M_w data reported by Clasen et al. for S in DEP.[49] By using the experimental scaling relation, c^* for S(48) was calculated to be 0.07 g/cm^3. In the sample 20% SI(16−16), the q^* for BCC at 90 °C is at 0.023 28 Å^{-1}. Using eq 1, the R_{mic} was calculated to be 16.5 nm. The edge length of a BCC unit cell is $4R_{mic}/\sqrt{3}$, and furthermore there are 2 micelles per BCC unit cell. Using this information, the packing fraction (ϕ_{crys}) of the BCC unit cell was calculated to be 0.68, which matches remarkably with the theoretical ϕ_{crys} of BCC unit cell. If we assume the micelles to be hard spheres and that the homopolymers are unable to penetrate the micelles, then the homopolymer effectively has only 32% of the unit cell available. Thus, we can define an effective homopolymer concentration c_{eff} as

$$c_{eff} = \frac{\phi\rho}{1 - \phi_{crys}} \tag{3}$$

where ϕ is the volume fraction of homopolymer in bulk solution and ρ is the polymer density. Using eq 3, for $\phi = 0.02$ and $\rho = 1.05$ g/cm^3, c_{eff} was calculated as 0.065 g/cm^3. Thus, we see that at $c_{eff}/c^* \approx 1.0$ the precipitous drop in ODT temperature begins. At about $c_{eff}/c^* \approx 1$, the crossover from dilute to semidilute regime also occurs, and the homopolymer chains begin overlapping with each other. Static light scattering experiments on polystyrene in DEP show that the inverse osmotic compressibility $\partial\pi/\partial c$ (and hence the osmotic pressure) increases as c/c^* of polymer increases in solution.[50] The osmotic pressure from the homopolymer chains plays a key role in the intermicellar attraction induced by polystyrene chains. In the framework of the AO model for hard spheres, the interparticle potential is given as

$$U(r) = \begin{cases} +\infty & r \le \sigma \\ -\Pi_0 V_0(r) & \sigma < r \le \sigma + 2R_g \\ 0 & r > \sigma + 2R_g \end{cases} \tag{4}$$

where σ is the hard-sphere radius of the particle, R_g is the radius of gyration of the homopolymer, V_0 is the overlapping depletion volume, and Π_0 is the osmotic pressure of the homopolymer chains. Thus, the strength of the attractive well is linked to the osmotic pressure of the homopolymer chains, which in turn is governed by the parameter c_{eff}/c^*. However, we note that the exact value of c_{eff}/c^* where T_{odt} starts decreasing may not be too significant. It is very difficult to calculate an accurate value of c_{eff} because from our experiments we have no knowledge about the location and conformation of the free homopolymer chains in these solutions. In eq 3 we ignore the overlapping of free polystyrene chains with the corona chains of the micelles. Thus, the calculated c_{eff}/c^* is only an estimate, where the value suggests that T_{ODT} drops when the homopolymer is close to a crossover over from dilute to semidilute regime.

A similar scaling argument was also proposed by Stiakakis et al., who studied the melting of an ultrasoft colloidal solid composed of multiarm stars, upon addition of homopolymer. An intriguing result was that when the plateau modulus and intrinsic viscosity of the gels were plotted as a function of c/c_h^*, all the data collapsed to produce a master curve. Here c_h^* is a reduced polymer concentration defined by $c_h^* = 3M_w/[4\pi N_{av}(R_h)^3]$, where R_h is the homopolymer hydrodynamic radius in dilute solution. Since the behavior of multiarm stars is analogous to spherical micelles, a similar scaling based on c/c^* was attempted in our system, too. By using the experimental data reported by Clasen et al., c^* for S(4), S(48), and S(180) was found to be 0.43, 0.07, and 0.026 g/cm^3, respectively. In Figure 7 a phase diagram was drawn where the x axis represents the ratio c/c^* and f_{PS} in the y axis represents the volume fraction of polystyrene in the diblock copolymer. The phase diagram remarkably captures all the important aspects of depletion interactions. From Figure 7 we observe that with increase in c/c^*, ordered phases are disordered and the BCC is replaced by the FCC phase. For the S(4) homopolymer, the c/c^* values are too low to cause any significant depletion effect. The parameter c/c^* essentially controls the osmotic pressure of the homopolymers acting on the spheres. The osmotic pressure depends on both the molecular weight and concentration of the homopolymer, and c/c^* thus provides a route to express those dependences in one scaling parameter.

Conclusion

In this paper we investigated the effects of addition of homopolymer on ordered solutions of SI diblocks in DEP. DEP is styrene-selective; hence, micelles with polyisoprene in the core and polystyrene in the corona are formed. Small-angle neutron scattering experiments performed previously in the SI + DEP system show that the addition of homopolymer generates attractive forces between the micelles. This phenomenon is analogous to depletion interactions observed in hard-sphere

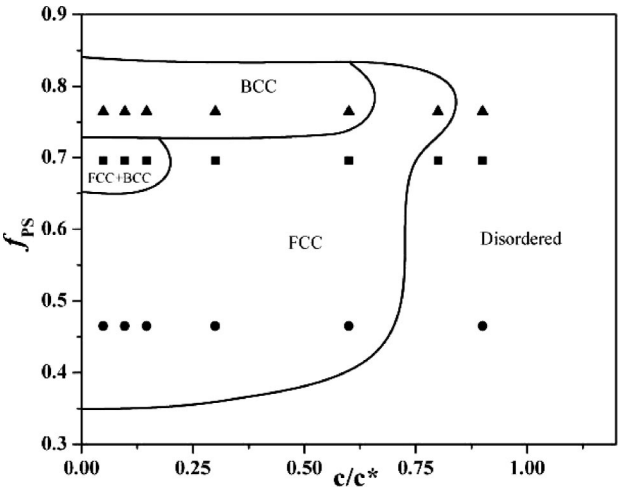

Figure 7. Influence of addition of homopolymer on the phase diagram of spherical micelles. The black dots represent data corresponding to SI(16−16) samples, filled squares represent SI(38−14), and upper triangles represent SI(50−13) data. Solid lines showing phase boundaries have been drawn as a guide to the eye.

colloidal systems. In concentrated solutions the micelles pack on to an FCC or BCC lattice. When homopolymer polystyrene is added to the solutions, the ordered phases are disordered. This phenomenon is universal in all samples and occurs irrespective of the morphology of the cubic phase. The results also show that in the presence of homopolymer FCC is favored over BCC and a phase sequence of BCC → FCC → disorder is observed. All of these phenomena are strongly dependent on the concentration and molecular weight of the homopolymer added. By calculating the micelle overall radius from the primary scattering peak, we concluded that N_{agg} of the micelles increases due to addition of homopolymer. The increase in N_{agg} occurs because the excluded volume interactions are screened in the corona of the micelles and the coronal chains contract. The reduction in the corona stretching and increase in N_{agg} results in a harder and short-ranged intermicellar interaction as a result of which the FCC phase is favored over the BCC phase. Furthermore, the attractive forces generated between micelles due to depletion interactions screens the intermicellar repulsive forces, thereby disordering the ordered phases.

The effect of temperature on the phase behavior of some samples with and without homopolymer was also investigated. One diblock went through an FCC−BCC OOT at higher temperature. On addition of an intermediate molecular weight homopolymer, the ODT temperature decreases and the FCC−BCC OOT temperature increases, as a result of which the BCC phase is edged out of the phase diagram. By calculating the effective concentration of the homopolymer in the solutions, we showed that the homopolymers are close to the chain overlap concentration when the drop in the ODT temperature begins. Finally, we attempted to organize the data on a phase diagram by using c/c^* of the homopolymer chains as a scaling parameter. This phase diagram captures all the essential aspects of the observed phase behavior. Overall, the results reported in the paper show that depletion interactions can be utilized as a new parameter to control the phase behavior of micelles, thereby further enriching the self-assembly toolbox of block copolymers in selective solvents.

Acknowledgment. This work was supported primarily by the MRSEC Program of the National Science Foundation (NSF) under Award DMR-0212302 and the University of Minnesota through a Doctoral Dissertation Fellowship (S.A.). Use of the Advanced Photon Source was supported by the U.S. Department of Energy, Basic Energy Sciences, Office of Science, under Contract W-31-109-Eng-38. Experiments were conducted at DND-CAT, which is supported by DuPont, Dow, NSF (DMR-9304725), and the Illinois Department of Commerce and Grant IBHE HECA NWU 96. Parts of this work were carried out in the Institute of Technology Characterization Facility, University of Minnesota, which receives partial support from NSF through the National Nanotechnology Infrastructure Network (NNIN) program.

Supporting Information Available: Figures of 1D scattering patterns and plots of elastic modulus versus temperature from rheology. This material is available free of charge via the Internet at http://pubs.acs.org.

References and Notes

(1) Riess, G. *Prog. Polym. Sci.* **2003**, *28*, 1107–1170.
(2) Hamley, I. W. *Block Copolymers in Solution: Fundamentals and Applications*; John Wiley & Sons, Ltd.: Chichester, 2005.
(3) Hanley, K. J.; Lodge, T. P.; Huang, C.-I. *Macromolecules* **2000**, *33*, 5918–5931.
(4) Lodge, T. P.; Pudil, B.; Hanley, K. J. *Macromolecules* **2002**, *35*, 4707–4717.
(5) Lodge, T. P.; Bang, J.; Park, M. J.; Char, K. *Phys. Rev. Lett.* **2004**, *92*, 145501.
(6) McConnell, G. A.; Gast, A. P.; Huang, J. S.; Smith, S. D. *Phys. Rev. Lett.* **1993**, *71*, 2102–2105.
(7) Lai, C.; Russel, W. B.; Register, R. A. *Macromolecules* **2002**, *35*, 841–849.
(8) Pople, J. A.; Hamley, I. W.; Fairclough, J. P. A.; Ryan, A. J.; Komanschek, B. U.; Gleeson, A. J.; Yu, G. E.; Booth, C. *Macromolecules* **1997**, *30*, 5721–5728.
(9) Hamley, I. W.; Mai, S.-M.; Ryan, A. J.; Fairclough, J. P. A.; Booth, C. *Phys. Chem. Chem. Phys.* **2001**, *3*, 2972–2980.
(10) Hamley, I. W.; Pople, J. A.; Diat, O. *Colloid Polym. Sci.* **1998**, *276*, 446–450.
(11) McConnell, G. A.; Lin, M. Y.; Gast, A. P. *Macromolecules* **1995**, *28*, 6754–6764.
(12) McConnell, G. A.; Gast, A. P. *Macromolecules* **1997**, *30*, 435–444.
(13) Imai, M.; Yoshida, I.; Iwaki, T.; Nakaya, K. *J. Chem. Phys.* **2005**, *122*, 044906.
(14) Ziherl, P.; Kamien, R. D. *Phys. Rev. Lett.* **2000**, *85*, 3528–3531.
(15) Abbas, S.; Lodge, T. P. *Phys. Rev. Lett.* **2006**, *97*, 097803.
(16) Abbas, S.; Lodge, T. P. *Langmuir* **2008**, *24*, 6247–6253.
(17) Asakura, S.; Osawa, F. *J. Chem. Phys.* **1954**, *22*, 1255–1256.
(18) Asakura, S.; Oosawa, F. *J. Polym. Sci.* **1958**, *33*, 183–192.
(19) Poon, W. C. K. *J Phys: Condens. Matter* **2002**, *14*, 859–880.
(20) Tuinier, R.; Rieger, J.; de Kruif, C. G. *Adv. Colloid Interface Sci.* **2003**, *103*, 1–31.
(21) Watanabe, H.; Kotaka, T. *J. Rheol.* **1983**, *27*, 223–240.
(22) Malmsten, M.; Lindman, B. *Macromolecules* **1993**, *26*, 1282–1286.
(23) Yamazaki, R.; Nose, T. *Polymer* **2003**, *44*, 6505–6511.
(24) Yamazaki, R.; Numasawa, N.; Nose, T. *Polymer* **2004**, *45*, 6227–6234.
(25) Renou, F.; Benyahia, L.; Nicolai, T. *Macromolecules* **2007**, *40*, 4626–4634.
(26) Stiakakis, E.; Vlassopoulos, D.; Likos, C. N.; Roovers, J.; Meier, G. *Phys. Rev. Lett.* **2002**, *89*, 208302.
(27) Stiakakis, E.; Vlassopoulos, D.; Roovers, J. *Langmuir* **2003**, *19*, 6645–6649.
(28) Stiakakis, E.; Petekidis, G.; Vlassopoulos, D.; Likos, C. N.; Iatrou, H.; Hadjichristidis, N.; Roovers, J. *Europhys. Lett.* **2005**, *72*, 664–670.
(29) Abbas, S.; Lodge, T. P. *Phys. Rev. Lett.* **2007**, *99*, 137802.
(30) Grason, G. M. *J. Chem. Phys.* **2007**, *126*, 114904.
(31) Hynninen, A.-P.; Dijkstra, M. *Phys. Rev. E* **2003**, *68*, 021407.
(32) Park, M. J.; Char, K.; Bang, J.; Lodge, T. P. *Langmuir* **2005**, *21*, 1403–1411.
(33) Abbas, S.; Lodge, T. P. Unpublished results.
(34) Ye, X.; Narayanan, T.; Tong, P.; Huang, J. S. *Phys. Rev. Lett.* **1996**, *76*, 4640–4643.
(35) Ye, X.; Narayanan, T.; Tong, P.; Huang, J. S.; Lin, M. Y.; Carvalho, B. L.; Fetters, L. J. *Phys. Rev. E* **1996**, *54*, 6500–6510.
(36) Lin, E. K.; Gast, A. P. *Macromolecules* **1996**, *29*, 390–397.
(37) Pierleoni, C.; Addison, C.; Hansen, J.-P.; Krakoviack, V. *Phys. Rev. Lett.* **2006**, *96*, 128302.
(38) Likos, C. N.; Mayer, C.; Stiakakis, E.; Petekidis, G. *J. Phys.: Condens. Matter* **2005**, *17*, S3363−S3369.
(39) Pham, K. N.; Puertas, A. M.; Bergenholtz, J.; Egelhaaf, S. U.; Moussaid, A.; Pusey, P. N.; Schofield, A. B.; Cates, M. E.; Fuchs, M.; Poon, W. C. K. *Science* **2002**, *296*, 104–106.

(40) Bang, J.; Viswanathan, K.; Lodge, T. P.; Park, M. J.; Char, K. *J. Chem. Phys.* **2004**, *121*, 11489–11500.
(41) Lee, L.-T.; Factor, B. J.; Kent, M. S.; Rondelez, F. *Phys. B (Amsterdam, Neth.)* **1996**, *221*, 320–324.
(42) Lee, L.-T.; Factor, B. J.; Rondelez, F.; Kent, M. S. *Faraday Discuss.* **1995**, *98*, 139–147.
(43) Lee, L.-T.; Kent, M. S. *Phys. Rev. Lett.* **1997**, *79*, 2899–2902.
(44) Wijmans, C. M.; Zhulina, E. B.; Fleer, G. J. *Macromolecules* **1994**, *27*, 3238–3248.
(45) Mortensen, K.; Batsberg, W.; Hvidt, S. *Macromolecules* **2008**, *41*, 1720–1727.
(46) Zhulina, E. B.; Adam, M.; LaRue, I.; Sheiko, S. S.; Rubinstein, M. *Macromolecules* **2005**, *38*, 5330–5351.
(47) Semenov, A. N. *Sov. Phys. JETP* **1985**, *61*, 733–742.
(48) Halperin, A. *Macromolecules* **1989**, *22*, 3806–3807.
(49) Clasen, C.; Plog, J. P.; Kulicke, W. M.; Owens, M.; Macosko, C.; Scriven, L. E.; Verani, M.; McKinley, G. H. *J. Rheol.* **2006**, *50*, 849–881.
(50) Wang, C. H.; Zhang, X. Q. *Macromolecules* **1993**, *26*, 707–714.

MA8013838